



저작자표시 2.0 대한민국

이용자는 아래의 조건을 따르는 경우에 한하여 자유롭게

- 이 저작물을 복제, 배포, 전송, 전시, 공연 및 방송할 수 있습니다.
- 이차적 저작물을 작성할 수 있습니다.
- 이 저작물을 영리 목적으로 이용할 수 있습니다.

다음과 같은 조건을 따라야 합니다:



저작자표시. 귀하는 원저작자를 표시하여야 합니다.

- 귀하는, 이 저작물의 재이용이나 배포의 경우, 이 저작물에 적용된 이용허락조건을 명확하게 나타내어야 합니다.
- 저작권자로부터 별도의 허가를 받으면 이러한 조건들은 적용되지 않습니다.

저작권법에 따른 이용자의 권리는 위의 내용에 의하여 영향을 받지 않습니다.

이것은 [이용허락규약\(Legal Code\)](#)을 이해하기 쉽게 요약한 것입니다.

[Disclaimer](#) 

의학박사 학위논문

세포내 protein phosphatase magnesium-
dependent 1A 는 파골세포 분화에 영향을 미
치며 축성 척추관절염의 질병 활성도와 관련
있음

Intracellular protein phosphatase magnesium-dependent 1A
negatively regulates osteoclast commitment and is associated
with disease activity of axial spondyloarthritis

울 산 대 학 교 대 학 원

의 학 과

권 오 찬

Intracellular protein phosphatase magnesium-
dependent 1A negatively regulates osteoclast
commitment and is associated with disease activity
of axial spondyloarthritis

지 도 교 수 유 빈

이 논문을 의학박사 학위 논문으로 제출함

2020 년 2 월

울 산 대 학 교 대 학 원

의 학 과

권 오 찬

권오찬의 의학박사학위 논문을 인준함

심사위원	유 빈	인
심사위원	이창근	인
심사위원	김용길	인
심사위원	오지선	인
심사위원	고은미	인

울 산 대 학 교 대 학 원

2020 년 2 월

Abstract

Objective: Increased protein phosphatase magnesium-dependent 1A (PPM1A) levels in patients with ankylosing spondylitis regulate osteoblast differentiation in bony ankylosis; however, the potential mechanisms that regulate osteoclast (OC) differentiation in relation to abnormal bone formation remain unclear. Therefore, in this study, conditional gene knockout (*PPM1A^{fl/fl};LysM-Cre*) mice were generated and their bone phenotypes were evaluated.

Methods: The bone phenotypes of *LysM-Cre* and *PPM1A^{fl/fl};LysM-Cre* mice were assessed via micro-computed tomography. OC differentiation was induced by culturing bone marrow-derived macrophages in the presence of the receptor activator of nuclear factor kappa-B (RANK) ligand and macrophage colony-stimulating factor (M-CSF) and was evaluated by counting tartrate-resistant acid phosphatase-positive multinucleated cells. The mRNA expressions of *PPM1A*, *RANK* and OC-specific genes were examined by quantitative real-time PCR, and protein levels were determined using Western blotting. Surface RANK expression was analyzed by fluorescent flow cytometry.

Results: The *PPM1A^{fl/fl};LysM-Cre* mice displayed reduced bone mass and increased OC differentiation and OC-specific gene expression compared with their *LysM-Cre* littermates. Mechanistically, reduced *PPM1A* function in OC precursors in *PPM1A^{fl/fl};LysM-Cre* mice induced OC lineage commitment by up-regulating RANK expression via p38 MAPK activation in response to M-CSF. PPM1A expression in macrophages was decreased by TLR4 activation. The ankylosing spondylitis disease activity score was negatively correlated with the expression of PPM1A in peripheral blood mononuclear cells from axial SpA patients.

Conclusion: The loss of *PPM1A* function in OC precursors driven by inflammatory signals contributes to OC lineage commitment and differentiation by elevating RANK expression, reflecting a potential role of PPM1A in dynamic bone metabolism in axial SpA.

Key words: Protein phosphatase magnesium-dependent 1A, Receptor activator of nuclear factor kappa-B, Osteoclast, Axial spondyloarthritis, Inflammation

Contents

Abstract.....	i
List of Tables and Figures	iv
Introduction.....	1
Materials and methods	5
Results	16
Discussion.....	33
Conclusion	38
References	39
국문 요약.....	48

List of Tables and Figures

Table 1. List of primers used in this study	10
Table 2. Characteristics of the 30 axial spondyloarthritis patients	32
Figure 1. Bone phenotype in <i>LysM-Cre</i> mice and <i>PPM1A^{fl/fl};LysM-Cre</i> mice	18
Figure 2. Decreased protein phosphatase magnesium-dependent 1A (PPM1A) expression in macrophages is associated with increased expression of osteoclast (OC)-specific genes and OC differentiation	20
Figure 3. The expression of <i>receptor activator of nuclear factor kappa-B (RANK)</i> was increased in macrophages from <i>PPM1A^{fl/fl};LysM-Cre</i> mice	24
Figure 4. Lipopolysaccharide (LPS) stimulation reduces protein phosphatase magnesium- dependent 1A (PPM1A) expression and increases receptor activator of nuclear factor kappa-B (RANK) expression in macrophages	27
Figure 5. Axial spondyloarthritis (axial SpA) patients with higher disease activity have lower expression levels of protein phosphatase magnesium-dependent 1A (PPM1A) in PBMCs	30

Introduction

Axial spondyloarthritis (axial SpA) is a chronic inflammatory disorder that primarily affects the axial skeleton, including the spine and sacroiliac joints.¹⁾ The characteristic features of axial SpA include new bone formation by the osteoproliferation of osteoblasts (OBs), which can eventually lead to bony ankylosis.¹⁾ Blocking the differentiation and activation of OBs prevented radiographic progression in a mouse model of ankylosing spondylitis (AS),²⁾ which illustrates that OBs represent an important component of bony ankylosis in AS. In addition, recent studies have focused on the divergent ability of osteoclast (OC) precursors to differentiate into OCs during OC commitment and accordingly influence the bone-resorbing capacity in AS.^{3,4)} Given that the bone remodeling process is coordinated by bone-resorbing OCs and bone-forming OBs,⁵⁾ the pathophysiological mechanisms underlying osteoproliferation in AS must be considered in terms of the coupling activities of OBs and OCs.^{2,3,6-8)}

Bone-resorbing OCs are derived from monocyte/macrophage precursors of the hematopoietic

progenitor lineage. Proliferating macrophages serve as OC precursors, which undergo further differentiation into OCs.⁹⁾ Two factors, namely macrophage colony-stimulating factor (M-CSF) and receptor activator of nuclear factor κ B (RANK) ligand (RANKL), are critical for OC lineage commitment and differentiation.¹⁰⁻¹²⁾ In the earlier stages of OC differentiation, M-CSF binds to its receptor c-fms on proliferating monocyte/macrophage precursors, thereby playing a key role in OC lineage commitment prior to OC differentiation¹³⁾ by activating transcription factors such as Mitf and PU.1.¹⁴⁾ Importantly, M-CSF can induce the expression of RANK, a receptor for RANKL, through mitogen-activated protein kinases (MAPKs) including p38, JNK and ERK.^{15,16)} This induction of RANK typifies OC lineage commitment. Following RANKL stimulation, the binding of TRAF6 to RANK results in the activation of MAPKs^{17,18)} and OC-specific transcription factors, such as NFATc1 and NF- κ B, to induce OC-specific genes,^{10,19-21)} leading to OC differentiation.^{9,22)} Therefore, in inflammatory conditions, the lineage commitment of macrophages is closely related to OC activity, resulting in pathological processes in bone remodeling in many diseases such as osteoporosis, rheumatoid arthritis (RA) and AS.^{3,4,23)}

Protein phosphatase magnesium-dependent 1A (PPM1A) is a member of the protein phosphatase 2C family of serine/threonine phosphatases.²⁴⁾ The expression of this protein is increased in cells or tissues under certain circumstances.^{25,26} Previous study demonstrated that PPM1A levels are increased in the synovial tissue of patients with AS and that its up-regulation enhances OB differentiation.²⁵⁾ Further, PPM1A expression is increased in macrophages during *Mycobacterium tuberculosis* infection, and this up-regulation plays a key role in the innate immune responses of macrophages.²⁶⁾ Considering that macrophages are the precursors of OCs⁹⁾ and that PPM1A is known to inactivate MAPKs by dephosphorylating p38 and JNK,²⁷⁾ which are critical for RANK expression,^{17,18)} PPM1A in macrophages might be a possible regulator of OC differentiation.

In this study, the down-regulation of the OC precursor macrophage-specific *PPM1A* in mice resulted in apparently increased osteoclastogenesis, which occurs through the regulation of RANK expression. The reverse correlation between AS disease activity score and expression level of PPM1A was also observed in peripheral blood mononuclear cells (PBMCs) obtained from patients with axial SpA. These discoveries establish PPM1A as a potential determinant

of OC lineage commitment from macrophages.

Materials and methods

Reagents and antibodies

RANKL and M-CSF were obtained from Pepro Tech Inc. (Rocky Hill, NJ, USA). A tartrate-resistant acid phosphatase (TRAP) Assay Kit, lipopolysaccharide (LPS from *Escherichia coli* O11:B4), PD98059, SB203580, SP60025 and β -actin antibodies were purchased from Sigma-Aldrich (St. Louis, MO, USA). Lipofectamine 2000 was purchased from Invitrogen (Grand Island, NY, USA). Anti-mouse CD265 (RANK)-phycoerythrin conjugate, protease and phosphatase inhibitor cocktails were purchased from Thermo Fisher Scientific Inc. (Rockford, IL, USA). Antibodies against PPM1A were purchased from Novus Biologicals (Littleton, CO, USA). Antibodies against p-ERK, ERK, p-p38, p38, p-JNK and JNK were purchased from Cell Signaling Technology (Danvers, MA, USA). All antibodies used in this study were polyclonal antibodies raised from rabbits.

Mice and bone mineral density (BMD) measurements and histological analysis

PPM1A^{fl^{ox}/fl^{ox}} (*PPM1A*^{fl/fl}, MGI:4458753, *Ppm1a*^{tm1a(EUCOMM)Hmgu}) mice were purchased from MRC Harwell (Oxfordshire, UK). To obtain mice with *PPM1A*-deficient macrophages, *PPM1A*^{fl/fl} mice were bred with *LysM-Cre* mice (004781, B6.129P2-Lyz2^{tm1(cre)If0}/J, Jackson Laboratory). *PPM1A*^{fl/fl};*LysM-Cre* mice were born at the expected Mendelian ratios, and they survived and reproduced as well as their wild-type (WT) littermates (*PPM1A*^{fl/fl} or *LysM-Cre* mice). *Toll-like receptor 4 (TLR4)* knockout (KO) mice were purchased from Jackson Laboratories (Bar Harbor, ME, USA). All mice in this study were from a pure C57BL/6 background. All animal procedures were approved by the Institutional Animal Care and Use Committee of the Asan Institute for Life Sciences in Seoul, Korea. Distal femurs dissected from the *LysM-Cre* mice and *PPM1A*^{fl/fl};*LysM-Cre* mice (n = 6 per group) were fixed in 4% paraformaldehyde. Bone volume was measured by a micro-CT analysis using the Skyscan 1072 system (14.85 μm pixel size, 50 kVp, 200 μA, 0.5 mm Al filter, Skyscan, Kontich, Belgium).²⁸⁾ Datasets were reconstructed using modified cone beam reconstruction software (NRecon) with a Feldkamp-based algorithm and were segmented into binary images using adaptive thresholding. After the acquisition of 200 tomographic slices, a bone volume analysis

was performed using CTan software (ver 1.6). BMD was measured in the region of interest with micro-CT (Skyscan). Areal BMD (g/cm³) in proximal femur (femoral neck, total hip) was measured using dual-energy X-ray absorptiometry (DXA; QDR 4500A, Hologic Inc., Waltham, MA). Three-dimensional surface-rendered models were generated using CTan software and visualized using CTVol (Bruker-micro-CT). The hindlimbs were dissected, fixed in 70% ethanol, embedded in methy methacrylate, and sectioned for histological analysis.²⁸⁾ Tissue sections were stained with hematoxylin eosin (H E) or TRAP with the Acid Phosphatase Assay Kit (Sigma Aldrich) in accordance with the manufacturer's instructions. TRAP staining indicates the presence of mature OCs. The OC surface was assessed on TRAP-stained sections using Image J densitometry software (Version 1.6, National Institutes of Health, Bethesda, MD).

Osteoclast differentiation

Bone marrow (BM) cells were isolated by flushing the marrow space in the femurs and tibiae collected from six-week-old C57BL6, *LysM-Cre*, *PPM1A^{fl/fl}* and *PPM1A^{fl/fl};LysM-Cre* mice.

Isolated cells were cultured for 12 h in α -minimal essential medium (α -MEM; Hyclone) supplemented with 10% FBS (Hyclone, Logan, UT) and 1% penicillin–streptomycin (Gibco, New York, NY). Non-adherent cells were collected after 12 h and cultured in petri dishes (Green Cross, Suwon, Korea) in the presence of M-CSF (30 ng/ml) for further 3 days. Adherent cells were considered to be bone marrow derived macrophages (BMMs) and were used as OC precursor cells. BMMs were cultured for 4 days with M-CSF (30 ng/ml) and RANKL (100 ng/ml) to induce differentiation into mature OCs. The medium was changed every 3 days. OC formation was evaluated by TRAP staining according to the manufacturer's instructions. The number of TRAP-positive multinucleated cells (MNCs; containing more than three nuclei, ten nuclei, or actin rings) was counted under a light microscope.²⁹⁾

Reverse transcription-polymerase chain reaction (RT-PCR) and quantitative real-time (qRT)-PCR analysis

Total RNA was isolated from the cells using Trizol Reagent (Life Technology, Carlsbad, CA, USA), and 0.5–1 μ g of RNA was reverse-transcribed using SuperScript II reverse transcriptase

(Life Technologies). The resulting cDNA was amplified by PCR using the primers shown in Table 1. The PCR conditions were as follows: denaturation at 95°C for 30 s, followed by annealing at 55°C~60°C for 30 s, and extension at 72°C for 1 min. The number of cycles fell within the range associated with linear amplification (23–34 cycles).²⁸⁾ qRT-PCR was performed using a Power SYBR Green 1-Step Kit and an ABI 7000 Real Time PCR System (Applied Biosystems, Carlsbad, CA, USA) according to the manufacturer's instructions.

Table 1. List of primers used in this study

Target	Sequences
mouse PPM1A	Forward 5'-ATG GTG CAG ATA GAA GCG GG-3'
	Reverse 5'-AGC CAG AGA GCC ATT GAC AC-3'
mouse DC-STAMP	Forward 5'-CCA AGG AGT CGT CCA TGA TT-3'
	Reverse 5'-GGC TGC TTT GAT CGT TTC TC-3'
mouse OC-STAMP	Forward 5'-TTC TCT GGC CTG GAG TTC CT-3'
	Reverse 5'-TGA CAA CTT AGG CTG GGC TG-3'
mouse CTSK	Forward 5'-AAT ACC TCC CTC TCG ATC CTA CA-3'
	Reverse 5'-GGT TCT TGA CTG GAG TAA CGT A-3'
mouse TRAP	Forward 5'-TCC TGG CTC AAA AAG CAG TT-3'
	Reverse 5'-ACA TAG CCC ACA CCG TTC TC-3'
mouse PU.1	Forward 5'-GAT GGA GAA GCT GAT GGC TTG G-3'
	Reverse 5'-TTC TTC ACC TCG CCT GTC TTG C-3'

mouse NFATc1	Forward 5'-GGG TCA GTG TGA CCG AAG AT-3'
	Reverse 5'-GGA AGT CAG AAG TGG GTG GA-3'
mouse c-fms	Forward 5'-CCC ACC CTG AAG TCC TGA GT-3'
	Reverse 5'-CTT TGT CCT AGG GAG ACG GC-3'
mouse RANK	Forward 5'-CAG ATG TCT TTT CGT CCA CAG A-3'
	Reverse 5'-AGA CTG GGC AGG TAA GCC T-3'
mouse GAPDH	Forward 5'-AGC CAC ATC GCTCAG ACA-3'
	Reverse 5'-GCC CAA TAC GAC CAA ATC C-3'
human PPM1A	Forward 5'-TGG CGT GTT GAA ATG GAG-3'
	Reverse 5'-AGC GGA TTA CTT GGT TTG TG-3'
human RANK	Forward 5'-AGA TCG CTC CTC CAT GTA CCA-3'
	Reverse 5'-GCC TTG CCT GTA TCA CAA ACT TT-3'
human GAPDH	Forward 5'-TGT TGC CAT CAA TGA CCC CTT-3'
	Reverse 5'-CTC CAC GAC GTA CTC AGC G-3'

DC-STAMP dendritic cell-specific transmembrane protein, *OC-STAMP* osteoclast stimulatory

transmembrane protein, *CTSK* cathepsin K, *NFATc1* nuclear factor of activated T cells c1,

GAPDH glyceraldehyde 3-phosphate dehydrogenase

Western blotting and fluorescent flow cytometry

Preparation of the cell lysates, SDS-PAGE gels and western blotting analyses were conducted according to a standard protocol.²⁸⁾ RANK expression on BMMs isolated from LysM-Cre and PPM1Afl/fl;LysM-Cre mice was evaluated by incubating 5×10^5 cells with phycoerythrin-conjugated anti-mouse RANK or an isotype control antibody in PBS containing 2% FBS at 4°C for 1 h. The cells were washed twice with PBS. Flow cytometry was performed on a FACScan according to the manufacturer's instructions (Becton Dickinson, San Jose, CA, USA).

Reporter assay

The RANK promoter-luciferase reporter plasmid was transiently transfected into BMMs from WT and TLR4 KO mice using Lipofectamine 2000 in accordance with the manufacturer's instructions. Two days after transfection, the cells were lysed using passive lysis buffer (Promega, Madison, WI, USA), and the luciferase activity in the extracts was measured using the dual luciferase assay system (Promega). Co-transfection with the Renilla vector allowed

normalization of the assays for differences in transfection efficiency.

Human samples

PBMCs were collected from patients with axial SpA (n = 30) and age- and sex-matched healthy controls (n = 13) at the Asan Medical Center (Seoul, Korea) and Hanyang University Hospital (Seoul, Korea). Clinical information was extracted from an electronic clinical database. All patients met the Assessment of SpondyloArthritis International Society classification criteria for axial SpA.³⁰⁾ Disease activity was determined using the ankylosing spondylitis disease activity score (ASDAS)-C reactive protein (CRP).³¹⁾ This study was approved by the Institutional Review Board of Asan Medical Center in Seoul, South Korea (IRB No: 2015-0274) and Hanyang University Hospital, Seoul, South Korea (IRB No: 2017-12-001).

Enzyme-linked immunosorbent assay (ELISA)

The concentrations of collagen type 1 cross-linked C-telopeptide (CTX, Mouse CTX-1 ELISA

kit, Novus, Centennial, CO, USA) in the plasma of *LysM-Cre* and *PPM1A^{fl/fl};LysM-Cre* mice were measured in accordance with the manufacturer's protocols. All samples were examined in triplicate for each experiment.

Statistical analysis

Differences between the two groups were analyzed using the Mann–Whitney U-test or an unpaired Student's t-test, and the differences amongst three groups were analyzed via one-way ANOVAs. The bars are triplicate averages from single experiments, and a representative of three independent experiments is shown. The relationships between parameters were tested using Spearman's rank correlation coefficient. Statistical analyses were considered significant for p values < 0.05.

Results

Macrophage-specific reduction of *PPM1A* expression in mice results in increased bone resorption due to enhanced OC formation

To evaluate the effect of reduced *PPM1A* expression in macrophage (OC precursors) on bone phenotype, *LysM-Cre* and *PPM1A^{fl/fl};LysM-Cre* mice were compared at six weeks of age.

Compared with *LysM-Cre* mice, the *PPM1A^{fl/fl};LysM-Cre* mice were smaller (Figure 1A). CT revealed sparse trabecular bone density in *PPM1A^{fl/fl};LysM-Cre* mice compared with *LysM-Cre* mice (Figure 1B). Accordingly, BMD, bone volume/total volume, trabecular (Tb) thickness and Tb number were significantly smaller and Tb spacing and the structure model index were significantly larger in *PPM1A^{fl/fl};LysM-Cre* mice, suggesting that bone resorption appears as a bone phenotype in *PPM1A^{fl/fl};LysM-Cre* mice (Figure 1C). TRAP staining revealed enhanced OC activity in *PPM1A^{fl/fl};LysM-Cre* mice, as evidenced by the increased positive staining of TRAP (Figure 1D). Indeed, the ELISA analysis revealed that the level of CTX in the plasma of *PPM1A^{fl/fl};LysM-Cre* mice was significantly higher than that of *LysM-*

Cre mice, indicating that the reduced bone mass in *PPM1A^{fl/fl};LysM-Cre* mice is caused by increased OC activity (Figure 1E).

Next, the expression status of OC-specific genes (*TRAP*, *DC-STAMP*, *OC-STAMP* and *CTSK*)^{10,19-21,32)} in macrophages from *PPM1A^{fl/fl};LysM-Cre* and *LysM-Cre* mice was evaluated.

RT-PCR revealed lower *PPM1A* expression in macrophages from *PPM1A^{fl/fl};LysM-Cre* mice than in C57BL/6, *LysM-Cre* and *PPM1A^{fl/fl}* mice, as expected (Figure 2A). Accordingly,

PPM1A protein expression in macrophages was similarly decreased in *PPM1A^{fl/fl};LysM-Cre* mice (Figure 2B). *TRAP*⁺ MNCs, which are OC-specific lineage cells,³³⁾ were numerically

increased in *PPM1A^{fl/fl};LysM-Cre* mice (Figure 2C and 2D). qRT-PCR illustrated that BMMs

in *PPM1A^{fl/fl};LysM-Cre* mice displayed higher *DC-STAMP*, *OC-STAMP*, *CTSK* and *TRAP* expression compared with that in *LysM-Cre* mice (Figure 2E). These data suggest that reduced

PPM1A expression in macrophages results in increased OC differentiation due to the increased capacity for OC formation in the early stages of OC differentiation.

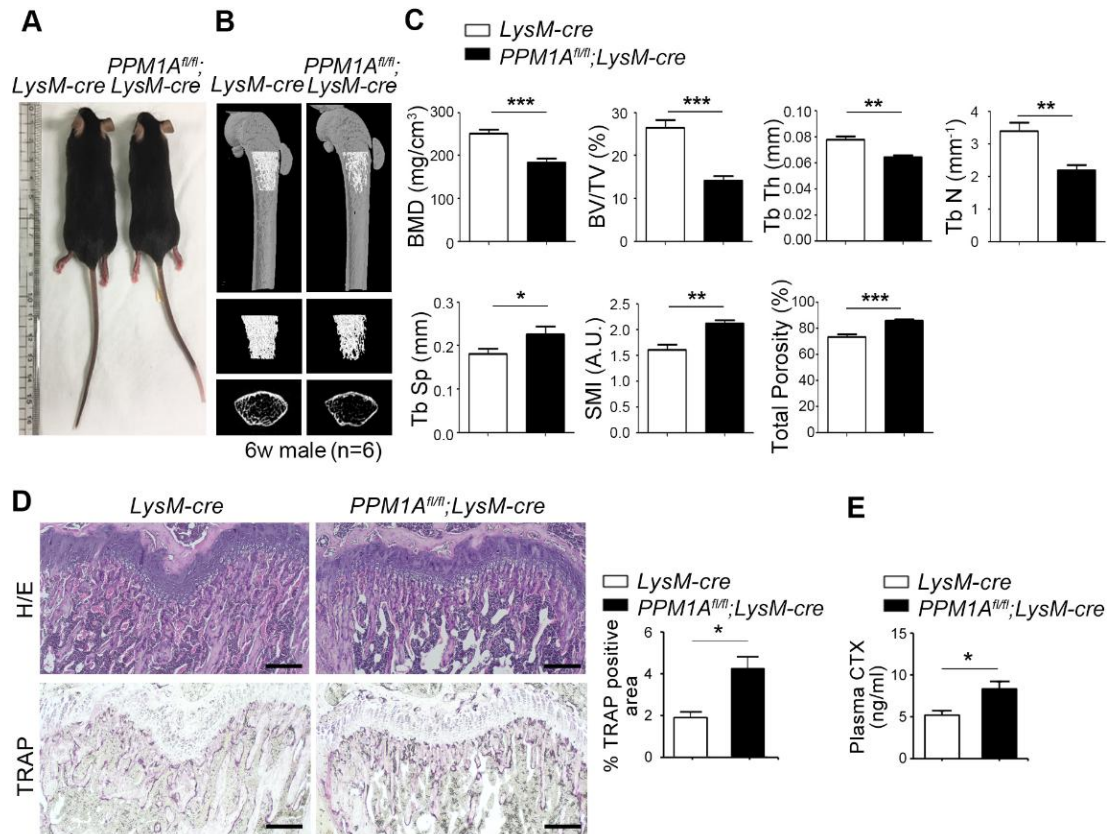


Figure 1. Bone phenotype in *LysM-Cre* mice and *PPM1A^{fl/fl};LysM-Cre* mice. A, Size comparison between *LysM-Cre* and *PPM1A^{fl/fl};LysM-Cre* mice. B, Comparison of trabecular bone density, as evaluated by micro-CT performed at six weeks of age, in male *LysM-Cre* and *PPM1A^{fl/fl};LysM-Cre* mice. The histograms represent three-dimensional structural parameters of the femurs. C, Quantification from B; Differences of bone density indices between *LysM-Cre* (n = 6) and *PPM1A^{fl/fl};LysM-Cre* mice (n = 6). Bone mineral density (BMD), bone volume per tissue volume (BV/TV), trabecular thickness (Tb. Th.), trabecular number (Tb. N.),

trabecular separation (Tb. Sp), structure model index (SMI), and total porosity (%). D, The hindlimbs were dissected, fixed and decalcified. The sections with the trabecular region were stained with hematoxylin-eosin (H-E) or tartrate-resistant acid phosphatase (TRAP, purple colour). Representative images from three independent experiments are shown. Scale bars, 200 μ m. Quantitation of TRAP-positive surface area. E, Collagen type 1 cross-linked C-telopeptide (CTX) in the plasma of from 6-week-old male *LysM-Cre* and *PPM1A^{fl/fl};LysM-Cre* mice was measured using an ELISA to represent bone turnover markers. Values are presented as the mean \pm SD. *: $p < 0.05$, **: $p < 0.01$, ***: $p < 0.001$ by the Mann-Whitney U test.

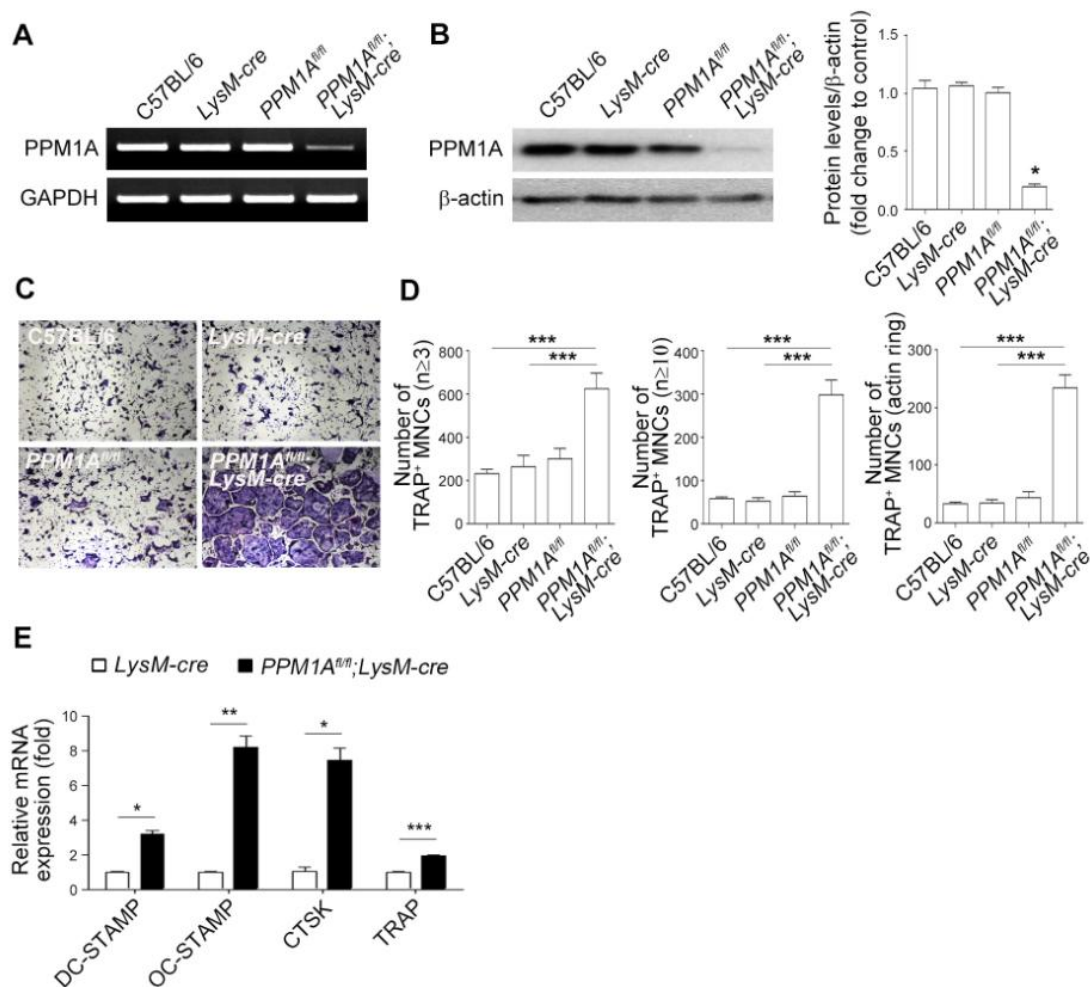


Figure 2. Decreased protein phosphatase magnesium-dependent 1A (PPM1A) expression in macrophages is associated with increased expression of osteoclast (OC)-specific genes and OC differentiation. A-B, *PPM1A* mRNA and protein expression levels in macrophages from C57BL/6, *LysM-Cre*, *PPM1A^{fl/fl}* and *PPM1A^{fl/fl};LysM-Cre* mice were determined using reverse transcription-polymerase chain reaction (RT-PCR) and western blotting (B, left). The densitometric quantification of PPM1A compared to β-actin is presented (B, right). GAPDH

and β -actin were used as the loading controls. C, Macrophages from C57BL/6, *LysM-Cre*, *PPM1A^{fl/fl}* and *PPM1A^{fl/fl};LysM-Cre* mice treated with macrophage colony-stimulating factor (30 ng/ml) and RANKL (100 ng/ml) for four days were fixed and stained with Tartrate-resistant acid phosphatase (TRAP) staining to detect OC formation. D, The numbers of TRAP⁺ multinucleated cells (MNCs) containing more than 3 ($n \geq 3$) or 10 nuclei ($n \geq 10$) or containing an actin ring from C were counted under a light microscope. E, Quantitative real-time polymerase chain reaction (qRT-PCR) analysis of OC-specific genes (*dendritic cell-specific transmembrane protein* [DC-STAMP] *osteoclast-specific transmembrane protein* [OC-STAMP], *cathepsin K* [CTSK] and *TRAP*) in bone marrow-derived macrophages (BMMs) in *LysM-Cre* and *PPM1A^{fl/fl};LysM-Cre* mice. The transcript levels were normalized to those of GAPDH. Values in B, D and E are presented as the mean \pm SD. *: $p < 0.05$, **: $p < 0.01$, ***: $p < 0.001$ by the Mann–Whitney U test.

***PPM1A* down-regulation in macrophages leads to increased expression of RANK via p38**

MAPK signaling

To determine the mechanism by which PPM1A influences OC commitment, the status of gene expression related to OC lineage commitment³⁴⁾ was investigated in M-CSF–cultured BMMs obtained from *LysM-Cre* and *PPM1A^{fl/fl};LysM-Cre* mice. Real-time PCR revealed that *PU.1* mRNA expression was increased in BMMs from *PPM1A^{fl/fl};LysM-Cre* mice with no alteration in *c-fms* expression, suggesting that the OC lineage commitment was enhanced by *PPM1A* down-regulation. Interestingly, *RANK* mRNA expression was increased in BMMs from *PPM1A^{fl/fl};LysM-Cre* mice (Figure 3A). RANK protein expression was increased in macrophages from *PPM1A^{fl/fl};LysM-Cre* mice compared with that in *LysM-Cre* mice (Figure 3B). Time-course Western blot analysis revealed no major changes in the activation of ERK, and JNK MAPKs upon M-CSF stimulation for 0–30 min compared with the *LysM-Cre* control (Figure 3C). Only p38 activation was increased in a time-dependent manner in *PPM1A^{fl/fl};LysM-Cre* macrophages compared with that in *LysM-Cre* macrophages (Figure 3C). To gain more direct evidence that PPM1A regulates *RANK* through p38 MAPK signaling,

BMMs were treated with various MAPKs inhibitors and RANK expression was analyzed by flow cytometry. Consistent with the up-regulation of *RANK*, there was a significant difference in RANK levels in *PPM1A^{fl/fl};LysM-Cre* macrophages due to the activation of p38 MAPK (Figure 3D). These data indicate that PPM1A influences RANK expression through the p38 signaling pathway and that it may directly dephosphorylate p38 MAPK, as previously reported.³⁵⁾ Taken together, PPM1A primarily regulates RANK expression in macrophages through the p38 signaling pathway.

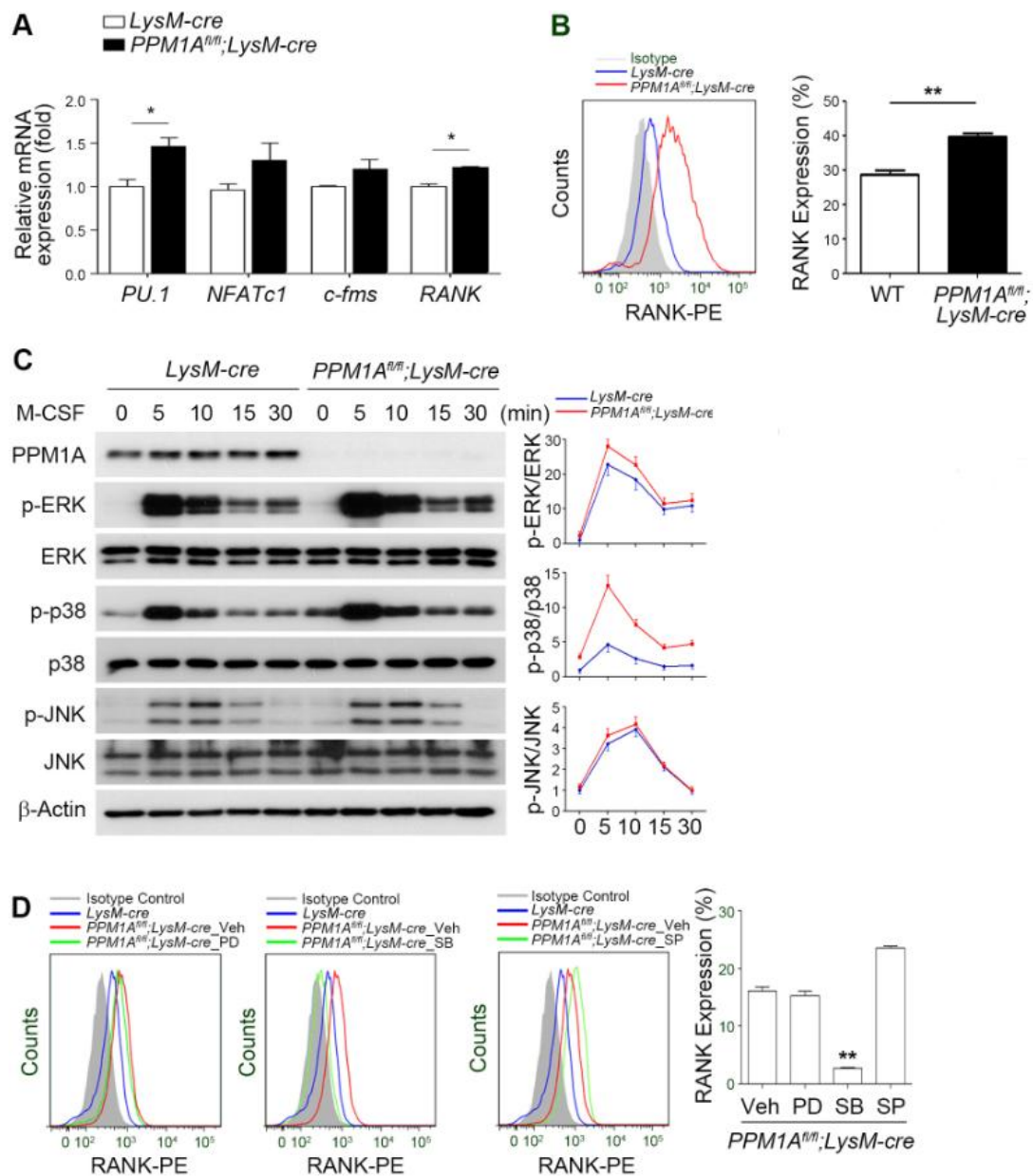


Figure 3. The expression of *receptor activator of nuclear factor kappa-B (RANK)* was increased in macrophages from *PPM1A^{fl/fl};LysM-Cre* mice. A, The mRNA expression levels of genes involved in macrophage colony-stimulating factor (M-CSF) signaling (*PU.1*, *NFATc1* and *c-fms*) and *RANK* in *LysM-Cre* and *PPM1A^{fl/fl};LysM-Cre* macrophages were determined

utilizing qRT-PCR. B, BMMs from *LysM-Cre* and *PPM1A^{fl/fl};LysM-Cre* mice were analyzed for RANK expression via fluorescent flow cytometry (left). The shaded histogram indicates the isotype control. The percentage of RANK-PE positive cells was quantified (right). C, Western blot analysis of M-CSF–induced mitogen-activated protein kinase (MAPK) activation (ERK, p38, JNK, p-ERK, p-p38, and p-JNK) in BMMs from *LysM-Cre* and *PPM1A^{fl/fl};LysM-Cre* mice after M-CSF stimulation for 0–30 min (left) and its quantification (right). D, BMMs from *LysM-Cre* and *PPM1A^{fl/fl};LysM-Cre* mice were pre-treated with DMSO (Veh), PD98059 (PD, 10 mM, ERK inhibitor), SB203580 (SB, 10 mM, p38 inhibitor) or SP60025 (SP, 10 mM, JNK inhibitor) in the presence of M-CSF and then analyzed for RANK expression by fluorescent flow cytometry (left). The percentage of RANK-PE positive cells was quantified (right). Values are presented as the mean \pm SD. *: $p < 0.05$, **: $p < 0.01$ by the Mann–Whitney U test.

Lipopolysaccharide (LPS) reduces PPM1A expression, resulting in increased RANK expression in macrophages

Next, the effect of inflammatory environment on PPM1A expression was explored. LPS, tumor necrosis factor α , interleukin (IL)-1 β and IL-6 were used as the inflammatory stimuli.

The mRNA and protein expression of *PPM1A* were diminished in macrophages following LPS stimulation (Figure 4A and 4B). Because TLR4 is the receptor for LPS,³⁶⁻³⁸⁾ it was then investigated whether PPM1A is down-regulated in response to LPS exposure using *TLR4* KO mice. Whereas LPS stimulation resulted in decreased *PPM1A* mRNA and protein expression in WT macrophages, these effects were not observed in macrophages from *TLR4* KO mice (Figure 4C and 4D). This regulatory axis affects RANK expression in macrophages, as evidenced by the finding that LPS stimulation increased *RANK* promoter activation (Figure 4E) and RANK expression in WT macrophages but not in *TLR4* KO macrophages (Figure 4F). Similarly, in human PBMCs, TLR4 activation by LPS stimulation was linked to decreased *PPM1A* mRNA expression, and this decrement was accompanied by an increase in *RANK* mRNA expression (Figure 4G).

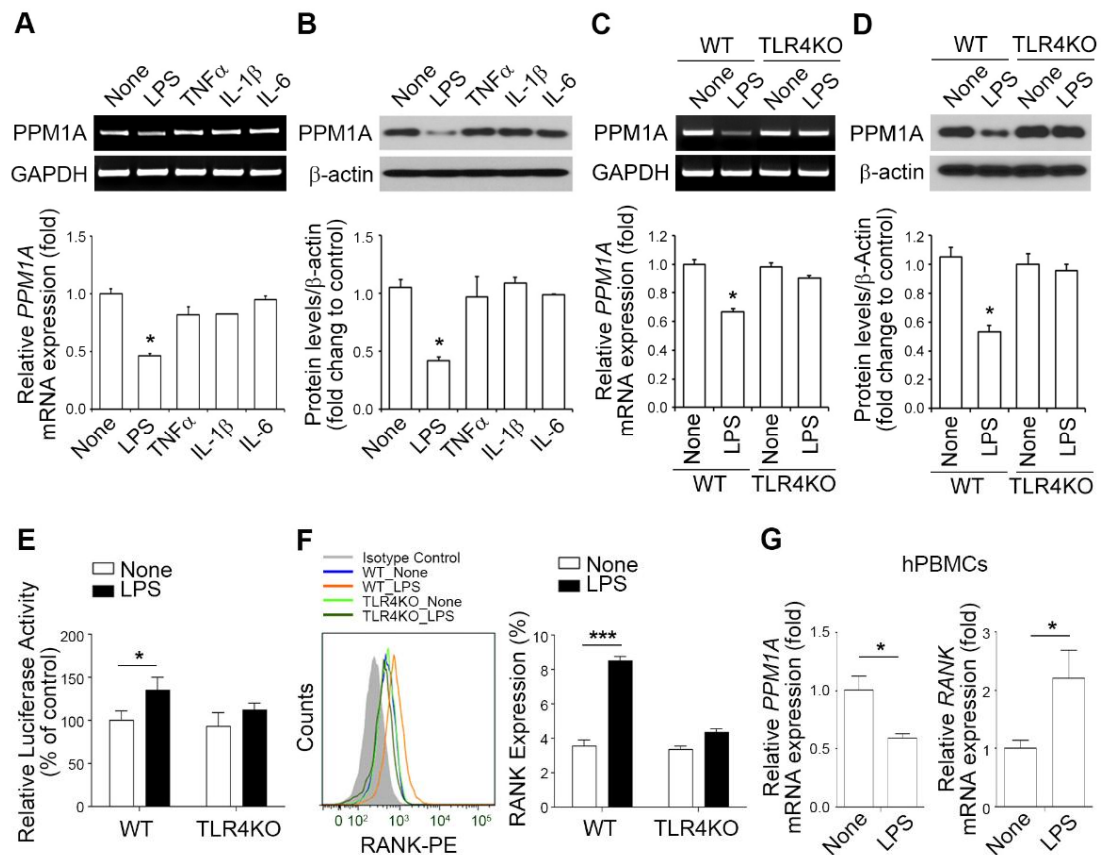


Figure 4. Lipopolysaccharide (LPS) stimulation reduces protein phosphatase magnesium-dependent 1A (PPM1A) expression and increases receptor activator of nuclear factor kappa-B (RANK) expression in macrophages. A, Macrophages were exposed to various inflammatory stimuli including LPS, tumor necrosis factor α (TNF α), interleukin (IL)-1 β and IL-6 and *PPM1A* mRNA expression was evaluated using RT-PCR (upper) and qRT-PCR (lower). B, PPM1A protein expression in macrophages treated with LPS, TNF α , IL-1 β and IL-6 was determined using western blot analysis (upper) and the quantification of protein expression is

presented (lower). C, *PPM1A* mRNA expression level in macrophages from wild-type (WT) and *Toll-like receptor 4 (TLR4)* knockout (KO) mice under LPS exposure was determined utilizing RT-PCR (upper) and qRT-PCR (lower). D, PPM1A protein expression level in WT and *TLR4* KO macrophages after LPS exposure was determined with western blotting (upper) and the protein expression is quantified (lower). E, BMMs from WT and *TLR4* KO mice were treated with LPS and RANK promoter-luciferase reporter plasmids were transiently transfected into these cells. After 24 h, the cells were harvested and subjected to the luciferase assay. The relative luciferase activity was normalized to the control activity. F, The surface RANK protein level in WT and *TLR4* KO BMMs exposed to LPS was determined by flow cytometry. G, PBMCs isolated from healthy controls were stimulated with LPS and *PPM1A* and *RANK* mRNA expression levels were determined by qRT-PCR. Values are presented as the mean \pm SD. *: $p < 0.05$, ***: $p < 0.001$ by the Mann–Whitney U test.

PPM1A expression in PBMCs from patients with axial spondyloarthritis

Because the results revealed a regulatory axis between PPM1A expression and the inflammatory condition, it was important to determine whether there is a correlation between PPM1A expression and disease activity in axial SpA.⁷⁾ The PPM1A/ β -actin ratio in PBMCs from axial SpA patients (n = 30) and age- and sex-matched healthy controls (n = 13) was compared and there was no significant difference in the PPM1A/ β -actin ratio between healthy controls and axial SpA patients (Figure 5A). Clinical variables of the axial SpA patients are shown in Table 2. Of the 30 axial SpA patients, 27 (90.0%) patients fulfilled the 1984 modified New York criteria for AS.³⁹⁾ Next, correlation between inflammatory burden, as measured by ASDAS-CRP, and PPM1A expression in PBMCs acquired from patients with axial SpA (Figure 5B) was evaluated. The PPM1A expressions in PBMCs and ASDAS-CRP were negatively correlated ($\gamma = -0.7072$, $p < 0.0001$), emphasizing that the inflammatory burden of axial SpA is associated with decreased PPM1A expression.

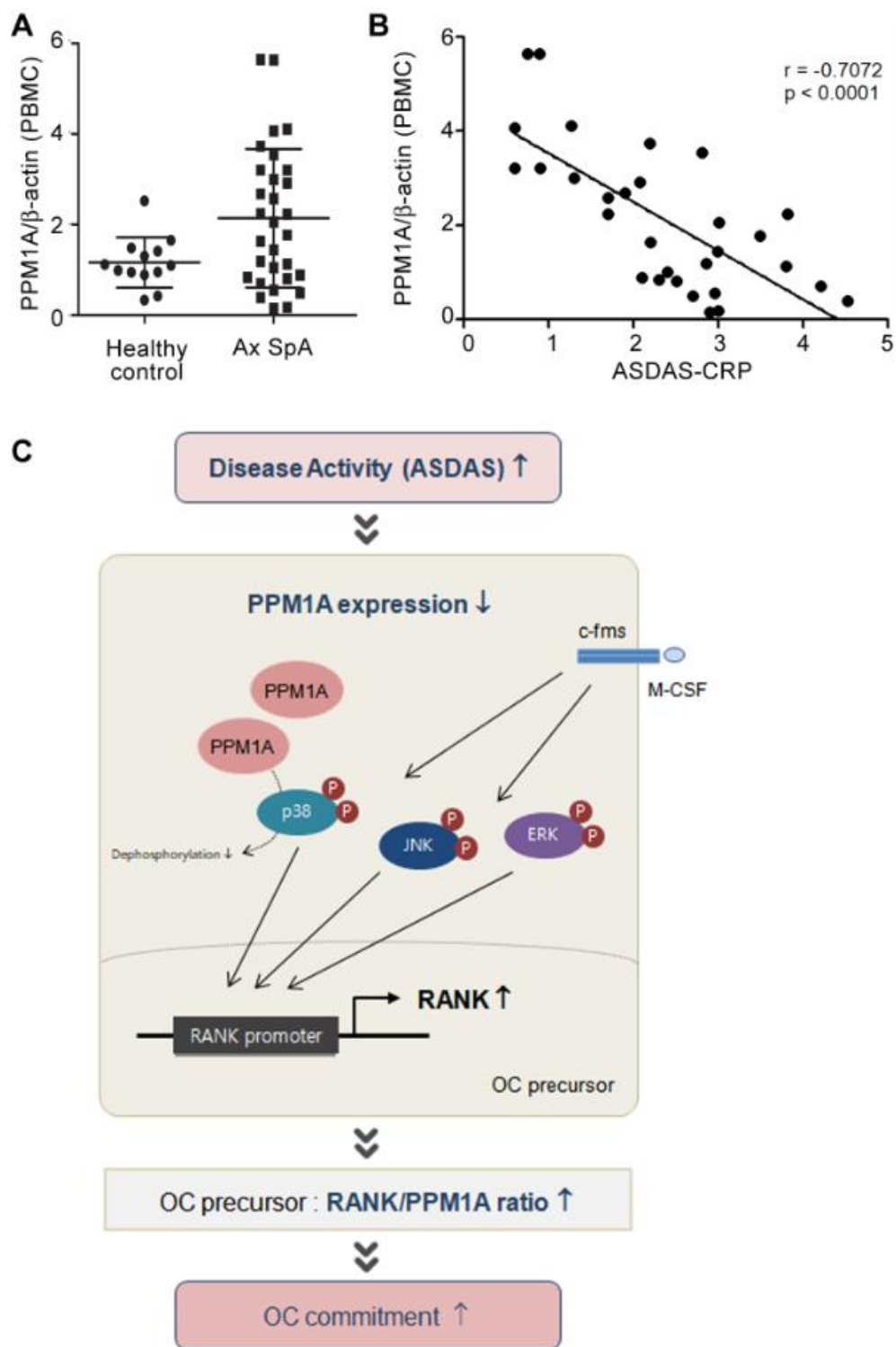


Figure 5. Axial spondyloarthritis (axial SpA) patients with higher disease activity have lower expression levels of protein phosphatase magnesium-dependent 1A (PPM1A) in PBMCs. A,

The protein levels of PPM1A and β -actin were measured using an immunoblot assay in PBMCs from axial SpA patients (n = 30) and age- and sex-matched healthy controls (n = 13).

B, Spearman's correlation analysis between PPM1A and ankylosing spondylitis disease activity score-C reactive protein (ASDAS-CRP) from axial SpA patients (n = 30). C, Suggested working model in axial SpA.

Table 2. Characteristics of the 30 axial spondyloarthritis patients

	N = 30
Age, median (IQR), years	33.0 (28.5–42.0)
Male, n (%)	28 (93.3)
Disease duration, median (IQR), months	19.2 (1.5–111.7)
HLA-B27 positive, n (%)	29 (96.7)
Ankylosing spondylitis ^a , n (%)	27 (90.0)
ASDAS-CRP, mean (\pm SD)	2.35 (\pm 1.06)

ASDAS-CRP; ankylosing spondylitis disease activity score-C reactive protein

^aPatients fulfilling the radiologic criterion of the 1984 modified New York criteria: sacroiliitis

grade ≥ 2 bilaterally or grade 3-4 unilaterally

Discussion

In this study, the macrophage-specific down-regulation of *PPM1A* results in OC commitment via increased RANK expression and enhanced RANK signaling. This is the first study to uncover the role of PPM1A in macrophages in OC differentiation. Previous study reported that PPM1A levels are increased in the synovial tissue of patients with AS and that PPM1A over-expression promoted OB differentiation.²⁵⁾ The serum levels of PPM1A in patients with AS were also increased compared with those in patients with RA and in healthy controls.²⁵⁾ Although the PPM1A serum levels varied amongst patients with AS, the clinical significance of this variability has not been determined. In this present study, a greater range of PPM1A expression was also observed in PBMCs from patients with axial SpA. Those with higher expression of PPM1A in PBMCs may attenuate RANK expression more potently, resulting in the inhibition of OC commitment and potential changes in the joint microstructure.

OCs are derived from hematopoietic stem cells (HSCs), and they are responsible for the resorption of endosteal bone surfaces and periosteal surfaces beneath the periosteum.^{10,40)}

RANK-RANKL is the primary factor involved in OC differentiation.^{9,22)} RANKL binds to RANK expressed on the surface of OC precursors and initiates downstream signaling (RANK signaling), which leads to the expression of OC-specific genes and consequently the differentiation and activation of mature OCs.^{9,22)} Thus, the RANK level in OC precursors can determine the capacity for OC formation through OC lineage commitment. As demonstrated in this study, *RANK* and *PU.1* mRNA expression was increased in *PPM1A^{fl/fl};LysM-Cre* macrophages compared with that in *LysM-Cre* macrophages. Considering that HSCs differentiate into OC precursors in the presence of PU.1 under M-CSF signaling,³³⁾ it can be concluded that macrophages from *PPM1A^{fl/fl};LysM-Cre* mice display enforced OC commitment due to M-CSF signaling. Notably, M-CSF, by binding to c-fms, autophosphorylates cytoplasmic tail tyrosine residues⁴¹⁾ and activates downstream events including p38 phosphorylation,^{42,43)} resulting in increased RANK expression in early OC precursors.⁴⁴⁾ Based on the present results, in circumstances where PPM1A expression is decreased in macrophages, p38 activity increases, resulting in increased RANK expression and thereby enhanced OC commitment.

The OC-specific genes that are induced by RANK-mediated intracellular signaling include *CTSK*, *TRAP*, calcitonin receptor, *DC-STAMP*, *OC-STAMP* and integrin $\beta 3$.^{10,19-21,32)} In the present data, the mRNA expression of *CTSK*, *TRAP*, *DC-STAMP* and *OC-STAMP* was increased in *PPM1A^{fl/fl};LysM-Cre* macrophages compared with that in *LysM-Cre* macrophages, indicating that PPM1A down-regulates OC-specific genes in these cells. Given that PPM1A inactivates MAPKs²⁷⁾ and that MAPKs are important mediators of RANK-mediated intracellular signaling,^{17,18)} PPM1A may attenuate further OC differentiation by down-regulating RANK-mediated intracellular signaling stimulated by RANKL in OC precursors. In particular, LPS stimulation reduced PPM1A expression in macrophages, thus identifying inflammation as an important variable affecting *PPM1A* mRNA expression. Thus, in inflammatory conditions, OC differentiation may be enhanced by increased RANK expression signaling attributable to PPM1A down-regulation in macrophages. However, the individual LPS-regulated inflammatory cytokines failed to suppress PPM1A. The reasons are not yet apparent but possibly there could be additional mediators about TLR4 signaling such as pathogen-associated molecular patterns rather than cytokine signaling that affects PPM1A.

In axial SpA, the severity of joint inflammation tends to fluctuate over time.⁴⁵⁾ Data in figure 5A show that there is no significant difference in the PPM1A expression in PBMCs from axial SpA patients vs. healthy controls. Due to the variability of disease activity of axial SpA, intracellular PPM1A expression in PBMCs from axial SpA patients may vary accordingly, rather than being constantly decreased or increased. This might be a possible explanation for the lack of significant difference in the PPM1A expression in PBMCs from axial SpA patients vs. healthy controls. A strong negative correlation was observed between ASDAS-CRP and PPM1A expression in PMBCs, supporting the inflammatory burden as an important regulator of PPM1A expression. Interestingly, elevated serum levels of soluble RANKL and increased bone resorption as assessed by decreased BMD have also been reported in patients with AS.⁴⁶⁾ In that study, prominent elevation of soluble RANKL in patients with AS might have led to OC commitment more actively in the presence of strong RANK expression in macrophages, thereby resulting in a resorptive bone phenotype. The notion that OCs play a role in the pathogenesis of AS is supported by the clinical benefits resulting from treatment with pamidronate in active AS.⁴⁷⁾ Taken together with the present results, the PPM1A level may

determine the resorptive bone phenotype in active axial SpA under an inflammatory burden
by altering the capacity for OC commitment in macrophages.

Conclusion

In conclusion, this study demonstrated that PPM1A down-regulation in macrophages results in RANK up-regulation and RANK signaling enhancement, causing OC commitment and further bone resorption. This finding suggests that PPM1A is both a potential enhancer of osteoblastogenesis²⁵⁾ and a potential regulator of OC commitment. Thus, in axial SpA with active inflammation, decreased PPM1A expression in PBMCs may enhance osteoclastogenesis via the up-regulation of RANK, thereby shifting the homeostasis of bone metabolism towards bone resorption (Figure 5B). These findings identify PPM1A as an important marker of bone metabolism in axial SpA and a potential therapeutic target for treating bony ankylosis.

References

1. Taurog JD, Chhabra A, Colbert RA. Ankylosing spondylitis and axial spondyloarthritis. *N Engl J Med* 2016;374:2563-74.
2. Lories RJ, Derese I, Luyten FP. Modulation of bone morphogenetic protein signaling inhibits the onset and progression of ankylosing enthesitis. *J Clin Invest* 2005;115:1571-9.
3. Perpetuo IP, Caetano-Lopes J, Vieira-Sousa E, Campanilho-Marques R, Ponte C, Canhao H, et al. Ankylosing spondylitis patients have impaired osteoclast gene expression in circulating osteoclast precursors. *Front Med (Lausanne)* 2017;4:5.
4. Perpetuo IP, Raposeiro R, Caetano-Lopes J, Vieira-Sousa E, Campanilho-Marques R, Ponte C, et al. Effect of tumor necrosis factor inhibitor therapy on osteoclast precursors in ankylosing spondylitis. *PLoS One* 2015;10:e0144655.
5. Khosla S. Pathogenesis of age-related bone loss in humans. *J Gerontol A Biol Sci Med Sci* 2013;68:1226-35.
6. Lories R. The balance of tissue repair and remodeling in chronic arthritis. *Nat Rev*

Rheumatol 2011;7:700-7.

7. Zhang X, Aubin JE, Inman RD. Molecular and cellular biology of new bone formation: insights into the ankylosis of ankylosing spondylitis. *Curr Opin Rheumatol* 2003;15:387-93.
8. Tam LS, Gu J, Yu D. Pathogenesis of ankylosing spondylitis. *Nat Rev Rheumatol* 2010;6:399-405.
9. Boyle WJ, Simonet WS, Lacey DL. Osteoclast differentiation and activation. *Nature* 2003;423:337-42.
10. Arai F, Miyamoto T, Ohneda O, Inada T, Sudo T, Brasel K, et al. Commitment and differentiation of osteoclast precursor cells by the sequential expression of c-Fms and receptor activator of nuclear factor kappaB (RANK) receptors. *J Exp Med* 1999;190:1741-54.
11. Cappellen D, Luong-Nguyen NH, Bongiovanni S, Grenet O, Wanke C, Susa M. Transcriptional program of mouse osteoclast differentiation governed by the macrophage colony-stimulating factor and the ligand for the receptor activator of

NFkappa B. J Biol Chem 2002;277:21971-82.

12. Dougall WC, Glaccum M, Charrier K, Rohrbach K, Brasel K, De Smedt T, et al.

RANK is essential for osteoclast and lymph node development. Genes Dev

1999;13:2412-24.
13. Tanaka S, Takahashi N, Udagawa N, Tamura T, Akatsu T, Stanley ER, et al.

Macrophage colony-stimulating factor is indispensable for both proliferation and

differentiation of osteoclast progenitors. J Clin Invest 1993;91:257-63.
14. Nakanishi A, Hie M, Iitsuka N, Tsukamoto I. A crucial role for reactive oxygen

species in macrophage colony-stimulating factor-induced RANK expression in

osteoclastic differentiation. Int J Mol Med 2013;31:874-80.
15. Lee K, Chung YH, Ahn H, Kim H, Rho J, Jeong D. Selective regulation of MAPK

signaling mediates RANKL-dependent osteoclast differentiation. Int J Biol Sci

2016;12:235-45.
16. Sobacchi C, Frattini A, Guerrini MM, Abinun M, Pangrazio A, Susani L, et al.

Osteoclast-poor human osteopetrosis due to mutations in the gene encoding RANKL.

Nat Genet 2007;39:960-2.

17. Li X, Udagawa N, Itoh K, Suda K, Murase Y, Nishihara T, et al. p38 MAPK-mediated signals are required for inducing osteoclast differentiation but not for osteoclast function. *Endocrinology* 2002;143:3105-13.
18. Matsumoto M, Sudo T, Saito T, Osada H, Tsujimoto M. Involvement of p38 mitogen-activated protein kinase signaling pathway in osteoclastogenesis mediated by receptor activator of NF-kappa B ligand (RANKL). *J Biol Chem* 2000;275:31155-61.
19. Wada T, Nakashima T, Hiroshi N, Penninger JM. RANKL-RANK signaling in osteoclastogenesis and bone disease. *Trends Mol Med* 2006;12:17-25.
20. Boyce BF. Advances in osteoclast biology reveal potential new drug targets and new roles for osteoclasts. *J Bone Miner Res* 2013;28:711-22.
21. Edwards JR, Mundy GR. Advances in osteoclast biology: old findings and new insights from mouse models. *Nat Rev Rheumatol* 2011;7:235-43.
22. Suda T, Takahashi N, Udagawa N, Jimi E, Gillespie MT, Martin TJ. Modulation of osteoclast differentiation and function by the new members of the tumor necrosis

- factor receptor and ligand families. *Endocr Rev* 1999;20:345-57.
23. Takayanagi H. Osteoimmunology: shared mechanisms and crosstalk between the immune and bone systems. *Nat Rev Immunol* 2007;7:292-304.
24. Zolnierowicz S. Type 2A protein phosphatase, the complex regulator of numerous signaling pathways. *Biochem Pharmacol* 2000;60:1225-35.
25. Kim YG, Sohn DH, Zhao X, Sokolove J, Lindstrom TM, Yoo B, et al. Role of protein phosphatase magnesium-dependent 1A and anti-protein phosphatase magnesium-dependent 1A autoantibodies in ankylosing spondylitis. *Arthritis Rheumatol* 2014;66:2793-803.
26. Sun J, Schaaf K, Duverger A, Wolschendorf F, Speer A, Wagner F, et al. Protein phosphatase, Mg^{2+}/Mn^{2+} -dependent 1A controls the innate antiviral and antibacterial response of macrophages during HIV-1 and *Mycobacterium tuberculosis* infection. *Oncotarget* 2016;7:15394-409.
27. Takekawa M, Maeda T, Saito H. Protein phosphatase 2C α inhibits the human stress-responsive p38 and JNK MAPK pathways. *EMBO J* 1998;17:4744-52.

28. Lee EJ, Kim SM, Choi B, Kim EY, Chung YH, Lee EJ, et al. Interleukin-32 gamma stimulates bone formation by increasing miR-29a in osteoblastic cells and prevents the development of osteoporosis. *Sci Rep* 2017;7:40240.
29. Lee EJ, Song DH, Kim YJ, Choi B, Chung YH, Kim SM, et al. PTX3 stimulates osteoclastogenesis by increasing osteoblast RANKL production. *J Cell Physiol* 2014;229:1744-52.
30. Rudwaleit M, van der Heijde D, Landewe R, Listing J, Akkoc N, Brandt J, et al. The development of Assessment of SpondyloArthritis international Society classification criteria for axial spondyloarthritis (part II): validation and final selection. *Ann Rheum Dis* 2009;68:777-83.
31. Lukas C, Landewe R, Sieper J, Dougados M, Davis J, Braun J, et al. Development of an ASAS-endorsed disease activity score (ASDAS) in patients with ankylosing spondylitis. *Ann Rheum Dis* 2009;68:18-24.
32. Lacey DL, Timms E, Tan HL, Kelley MJ, Dunstan CR, Burgess T, et al. Osteoprotegerin ligand is a cytokine that regulates osteoclast differentiation and

activation. *Cell* 1998;93:165-76.

33. Amarasekara DS, Yun H, Kim S, Lee N, Kim H, Rho J. Regulation of osteoclast differentiation by cytokine networks. *Immune Netw* 2018;18:e8.
34. Boyce BF. Advances in the regulation of osteoclasts and osteoclast functions. *J Dent Res* 2013;92:860-7.
35. Dvashi Z, Sar Shalom H, Shohat M, Ben-Meir D, Ferber S, Satchi-Fainaro R, et al. Protein phosphatase magnesium dependent 1A governs the wound healing-inflammation-angiogenesis cross talk on injury. *Am J Pathol* 2014;184:2936-50.
36. Poltorak A, He X, Smirnova I, Liu MY, Van Huffel C, Du X, et al. Defective LPS signaling in C3H/HeJ and C57BL/10ScCr mice: mutations in Tlr4 gene. *Science* 1998;282:2085-8.
37. Qureshi ST, Lariviere L, Leveque G, Clermont S, Moore KJ, Gros P, et al. Endotoxin-tolerant mice have mutations in Toll-like receptor 4 (Tlr4). *J Exp Med* 1999;189:615-25.
38. Hoshino K, Takeuchi O, Kawai T, Sanjo H, Ogawa T, Takeda Y, et al. Cutting edge:

- Toll-like receptor 4 (TLR4)-deficient mice are hyporesponsive to lipopolysaccharide: evidence for TLR4 as the Lps gene product. *J Immunol* 1999;162:3749-52.
39. van der Linden S, Valkenburg HA, Cats A. Evaluation of diagnostic criteria for ankylosing spondylitis. A proposal for modification of the New York criteria. *Arthritis Rheum* 1984;27:361-8.
 40. Zaidi M. Skeletal remodeling in health and disease. *Nat Med* 2007;13:791-801.
 41. Feng X, Takeshita S, Namba N, Wei S, Teitelbaum SL, Ross FP. Tyrosines 559 and 807 in the cytoplasmic tail of the macrophage colony-stimulating factor receptor play distinct roles in osteoclast differentiation and function. *Endocrinology* 2002;143:4868-74.
 42. Wang Y, Piper MG, Marsh CB. The role of Src family kinases in mediating M-CSF receptor signaling and monocytic cell survival. *Adv Biosci Biotechnol* 2012;3:592-602.
 43. Wang Y, Zeigler MM, Lam GK, Hunter MG, Eubank TD, Khramtsov VV, et al. The role of the NADPH oxidase complex, p38 MAPK, and Akt in regulating human

- monocyte/macrophage survival. *Am J Respir Cell Mol Biol* 2007;36:68-77.
44. Soysa NS, Alles N, Aoki K, Ohya K. Osteoclast formation and differentiation: an overview. *J Med Dent Sci* 2012;59:65-74.
 45. Stone MA, Pomeroy E, Keat A, Sengupta R, Hickey S, Dieppe P, et al. Assessment of the impact of flares in ankylosing spondylitis disease activity using the Flare Illustration. *Rheumatology (Oxford)* 2008;47:1213-8.
 46. Kim HR, Lee SH, Kim HY. Elevated serum levels of soluble receptor activator of nuclear factors-kappaB ligand (sRANKL) and reduced bone mineral density in patients with ankylosing spondylitis (AS). *Rheumatology (Oxford)* 2006;45:1197-200.
 47. Maksymowych WP, Jhangri GS, Fitzgerald AA, LeClercq S, Chiu P, Yan A, et al. A six-month randomized, controlled, double-blind, dose-response comparison of intravenous pamidronate (60 mg versus 10 mg) in the treatment of nonsteroidal antiinflammatory drug-refractory ankylosing spondylitis. *Arthritis Rheum* 2002;46:766-73.

국문요약

목표: 강직성 척추염 환자의 혈청과 활막에서 protein phosphatase magnesium-dependent 1A (PPM1A)는 증가되어 있으며, 이는 조골세포 분화를 촉진하여 비정상적인 골 형성, 즉, 뼈의 강직을 유발한다. 그러나 비정상적인 골 형성과 관련하여 파골세포 분화가 어떻게 조절되는지에 대해서는 잘 알려져 있지 않다. 본 연구에서는 조건부 유전자 knockout ($PPM1A^{fl/fl};LysM-Cre$) 쥐를 이용하여 그들의 골 표현형을 확인하고, 파골세포 분화가 어떤 기전으로 조절되는지 보고자 한다.

연구방법: $LysM-Cre$ 쥐와 $PPM1A^{fl/fl};LysM-Cre$ 쥐의 골 표현형을 micro-computed tomography 를 이용하여 평가하였다. 파골세포의 분화는 nuclear factor kappa-B (RANK) ligand 와 macrophage colony-stimulating factor (M-CSF)의 존재 하에 골수 유래 대식세포를 배양함으로써 유도하였고, tartrate-resistant acid phosphatase-양성인 다핵세포를 계수함으로써 평가하였다. $PPM1A$, $RANK$ 및 파골세포 특이적 유전자의 mRNA 발현은 정량적 실시간 PCR 을 통해 측정하였고, 단백질 발현은 Western blotting 을 이용하여 측정하였다.

결과: *PPM1A^{fl/fl};LysM-Cre* 쥐는 *LysM-Cre* 쥐에 비해 골 질량이 감소되어 있었고, 파골세포 분화 및 파골세포 특이적 유전자의 발현이 증가되어 있었다. 기전상으로 *PPM1A^{fl/fl};LysM-Cre* 쥐의 대식세포에서의 *PPM1A* 기능 감소는 p38 MAPK 활성화를 통해 RANK 발현을 증가시킴으로써 파골세포로의 분화를 유도하였다. 염증성 자극이 PPM1A 발현에 미치는 영향을 확인한 결과, 대식세포에서의 PPM1A 발현은 염증성 자극에 의한 TLR4 활성화에 의해 감소되었다. 더 나아가 축성 척추관절염 환자의 질병활성도와 말초 혈액 단핵 세포에서의 PPM1A 발현 정도 사이에도 음의 상관 관계를 보였다.

결론: 염증성 자극에 의한 대식세포에서의 *PPM1A* 기능 손실은 RANK 발현을 증가시키며 파골세포의 분화에 기여한다. 축성 척추관절염의 골 대사에 있어 PPM1A는 중요한 역할을 하는 것으로 생각된다.

중심 단어: Protein phosphatase magnesium-dependent 1A, Receptor activator of nuclear factor kappa-B, 파골세포, 축성 척추관절염, 염증